

# The Formation and Characterization of Nanocrystalline Phases by Mechanical Milling of Biphasic Calcium Phosphate/Poly-L-Lactide Biocomposite

I. Nikčević<sup>1</sup>, D. Maravić<sup>2</sup>, N. Ignjatović<sup>1</sup>, M. Mitrić<sup>2</sup>, D. Makovec<sup>3</sup> and D. Uskoković<sup>1</sup>

<sup>1</sup>*Institute of Technical Sciences of the Serbian Academy of Sciences and Arts, Belgrade, Serbia*

<sup>2</sup>*The Vinča Institute of Nuclear Sciences, Belgrade, Serbia*

<sup>3</sup>*Jožef Stefan Institute, Jamova 39, SI-1000 Ljubljana, Slovenia*

Biphasic calcium phosphate/poly-L-lactide granules of 150–200 μm sizes were subjected to high-energy mechanical milling in a planetary ball mill for up to 480 minutes. Characterization of the material obtained was carried out using X-ray diffraction (XRD), differential scanning calorimetry (DSC), environmentally scanning electronic microscopy (ESEM), transmission electron microscopy (TEM) and infrared spectroscopy (IR). These techniques confirmed that mechanical milling induced significant changes in the biocomposite structure and properties. The most significant changes are reduction of the HAp crystallites size from 99.8 to 26.7 nm and β-TCP from 97.3 to 29.6, as well as crystallinity of PLLA phases. Homogeneous phase distribution (arrangement) is obtained by extending the duration of mechanical milling. [doi:10.2320/matertrans.47.2980]

(Received May 15, 2006; Accepted October 2, 2006; Published December 15, 2006)

**Keywords:** nanostructured biocomposite, biphasic calcium phosphate, poly-L-lactide, mechanical milling, size of crystallites, crystallinity degree

## 1. Introduction

Ceramic/polymer composites play a significant role in bone reparations, as their properties are very similar to natural bone tissue.<sup>1)</sup> Calcium hydroxyapatite/poly-L-lactide (HAp/PLLA) composite biomaterial belongs to this group of composites that can be successfully implemented in bone tissue repairation due to their osteoconductive and biocompatible properties.<sup>2–4)</sup> HAp/PLLA consists of a bio-nonresorbable ceramic component (hydroxyapatite, HAp) and a bioresorbable polymer component (poly-L-lactide, PLLA). The structure of the HAp/polymer composite closely imitates natural bone tissues,<sup>5)</sup> that enable the successful application of this composite as bone substitute material. However, the work on achieving a better compatibility in mechanical properties is still in progress. Besides biocompatibility, a response from the living organism to an applied implant depends on various factors such as porosity, surface microstructure, elastic modules, compressive strength, etc.<sup>6–8)</sup> Addition of biphasic calcium phosphate (BCP) to polymers can significantly improve the polymer bioactivity,<sup>9)</sup> while BCP itself can be an exceptional carrier of growth factors which facilitates its wider application in medicine and dentistry.<sup>10)</sup> Low content of β-tricalcium phosphate, β-TCP in BCP assists the rapid bonding of bone substitutes to natural bones via rapid dissolution of β-TCP. However, excess content of β-TCP in BCP lowers the mechanical properties and chemical stability of bone substitutes. If the BCP component in the composite is highly crystalline then it is bio-nonresorbable and vice versa.<sup>11–14)</sup> It can be said that bioresorption is initiated in the amorphous regions of PLLA. Therefore, when BCP is highly crystalline, the time of biocomposite bioresorption depends on the crystallinity/amorphous ratio in PLLA.<sup>15,16)</sup>

High-energy mechanical milling is a technique for producing a homogeneous powder, with fine microstructure,

by milling a powder mixture.<sup>16–18)</sup> The most typical characteristic of mechanical milling is the decreased crystallite size. Some materials become amorphous by milling, while others show the decrease of crystallite size to a minimal value which is characteristic for a given material.<sup>19,20)</sup> HAp or BCP with other bioresorbable polymers has already been studied as well as mechanochemical synthesis of HAp,<sup>21–26)</sup> while high energy mechanical processing of composite BCP/PLLA has not been investigated.

This article examines the possible influence of mechanical milling on some properties of BCP/PLLA biocomposite. The influence of the milling time on crystallite size of BCP, on melting temperature, and crystallinity of the polymer has been defined. The influence of the mechanical milling on microstructure evaluation was analyzed by ESEM and TEM analysis. Qualitative stability of the biocomposite during mechanical treatment was defined by IR spectroscopy.

## 2. Experimental Procedure

Calcium phosphate was synthesized by a reaction of Ca(NO<sub>3</sub>)<sub>2</sub> with (NH<sub>4</sub>)<sub>3</sub>PO<sub>4</sub> in solution. To a solution of Ca(NO<sub>3</sub>)<sub>2</sub>, vigorously mixed by a magnetic stirrer with a rate of 100 rpm/min, a solution of (NH<sub>4</sub>)<sub>3</sub>PO<sub>4</sub> was added for 180 min. The obtained suspension was heated to boiling, and the precipitate, being held in the starting solution for 18 h, was separated by filtration using a Büchner's funnel. The obtained filter cake was washed with warm distilled water till the ammonia smell dissipated. The pH of the solution was maintained above 10 by adding ammonia due to the stability of calcium phosphate. The obtained filter cake was dried in vacuum at room temperature ( $P = 10$  Pa), reducing the water content to approximately 30%. By straining partially dried gel through plastic sieves of a mesh, spherical granules were obtained, and dried at room temperature. The dried granules were calcined at 1100°C

for 6 h.<sup>2)</sup> The calcium phosphate/PLLA ratio in all samples was 80 : 20. The PLLA fraction of 20 mass% represents a volume fraction of 41%. Natural bone tissue consists of 60 vol% of the inorganic phase while the remaining 40 vol% is connective tissue (of polymer nature). By BCP to PLLA weight ratio in the composite material, the concept of natural bone is preserved.<sup>2)</sup>

The polymeric component, a commercial PLLA (Fluka, Germany,  $M_w = 100000$ ), was completely dissolved in chloroform. Biphasic calcium phosphate granules, BCP (containing 80 mass% HAp and 20 mass% of  $\beta$ -tricalcium phosphate,  $\beta$ -TCP) were added to the PLLA-chloroform solution. The degradation rate of TCP is 3–12 times higher than that of HAp. Partial degradation of calcium phosphates encourages the bonding of bone to the ceramic. Biphasic calcium phosphates (BCP), a mixture of HAp and TCP in a ratio of 8 : 2, is the most promising because it may enhance the bioactivity, because it combines the reactivity of TCP and the stability of HA.<sup>27)</sup> The average size of the granules of BCP was 150–200  $\mu\text{m}$ . The obtained mixture was dried in a vacuum, until the solvent completely evaporated. The mixture contained 80% BCP and 20% PLLA. Derived powders were put in the agate vessels with balls of alumina. Mechanical milling was carried out in a planetary mill (RETC model PM4), having an angle velocity of 100 rpm in air atmosphere. The milling was completed after 8 h. The samples were taken before treatment and 5, 15, 30, 60, 240 and 480 min after treatment.

Phases present in the samples were analyzed by X-ray diffractometer (Phillips 1010), using  $\text{Cu-K}\alpha_{1,2}$  radiation (0.15418 nm), in the range of  $2\theta$  from 9–67° with step increments of 0.05°, and the time of exposure was 2 s/step. Average crystallite sizes were determined using Debye-Scherrer formula. Cell parameters were evaluated from appropriate peak positions.

DSC measurements were made by a Perkin Elmer Model DSC-2 differential scanning calorimeter. The average mass of samples was 3.0 mg. They were analyzed in a nitrogen atmosphere and heated from 305 to 485 K (heating rate of 20  $\text{K min}^{-1}$ ). The PLLA melting temperature ( $T_m$ ), crystallization temperature ( $T_c$ ), crystallization enthalpy ( $\Delta H_c$ ) and melting enthalpy ( $\Delta H_m$ ) were calculated.

The microstructure of the surface morphology of BCP/PLLA composite was observed by, environmental scanning electronic microscope (ESEM), XL 30 (FEI Company, Hillsboro, Oregon).

To accomplish more detailed analysis of BCP/PLLA composite particle morphology, transmission electronic microscopy, TEM (JEOL JEM 2000 FX) was used with an acceleration voltage of 200 keV. BCP/PLLA samples were dispersed in acetone using ultrasound and the suspensions were deposited on a copper grid-supported transparent carbon foil.

Phase analysis of the product sample was carried out using IR spectroscopy, KBr pellet technique. Samples of BCP, PLLA, and BCP/PLLA were analyzed by a Perkin Elmer 983G spectrophotometer, in the range of 4000–250  $\text{cm}^{-1}$  of the IR spectrum. Constituent components were analyzed under the same conditions.

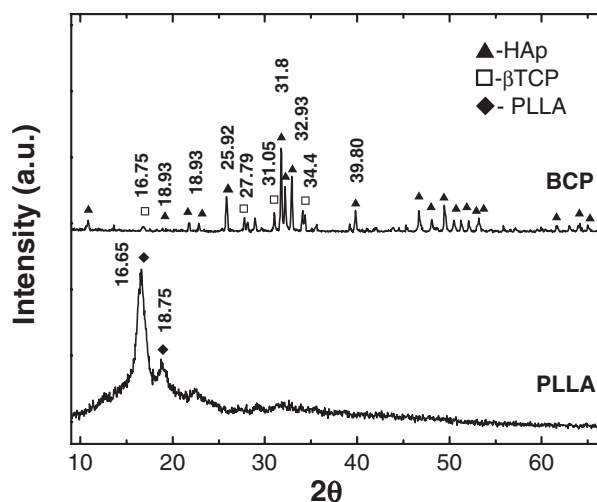


Fig. 1 The diffractogram of starting samples BCP and PLLA.

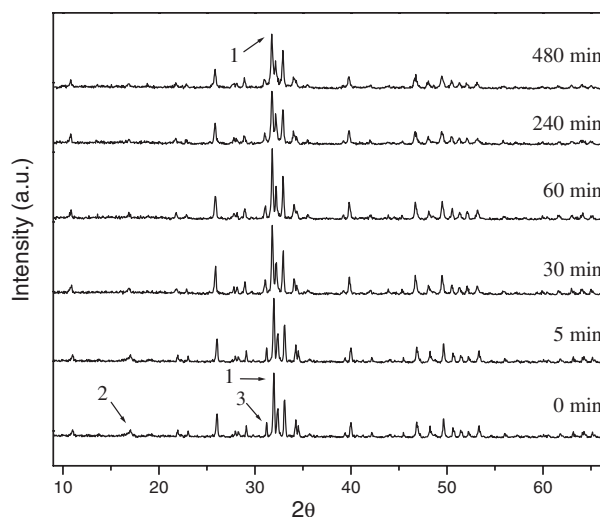


Fig. 2 Comparative X-ray diffractograms of the BCP/PLLA composite samples taken before and during the milling.

### 3. Results and Discussion

#### 3.1 X-ray diffraction analysis (XRD)

Effects of the mechanical milling on the structure of the biocomposite were analyzed by X-ray diffraction. Diffractograms of starting samples of BCP and PLLA are shown in Fig. 1. The results of XRD measurements on the samples after each sampling period of the mechanical processing are shown in Fig. 2.

All obtained diffractograms have a region that is characteristic for HAp (1) (JCPDS file no. 09-432)<sup>28)</sup> and for  $\beta$ -TCP (3) (JCPDS file no. 09-169).<sup>29)</sup> In addition, the most intensive diffraction maximum characteristic for PLLA (2) at  $2\theta = 17^\circ$  overlaps the diffraction peak characteristic for  $\beta$ -TCP (110) and the diffraction peak at  $2\theta = 19^\circ$  overlaps the diffraction peak characteristic for HAp (110). Peak broadening at  $2\theta = 17^\circ$  with increasing milling time implies PLLA crystallinity change.

Since the BCP/PLLA mixture contains a relatively small amount of PLLA, the corresponding diffraction maxima of

Table 1 Cell parameters and crystallite size of the ceramic component in BCP/PLLA.

Milling time (min)	<i>a</i> (nm)		<i>c</i> (nm)		<i>cs</i> (nm)	
	HAp	$\beta$ -TCP	HAp	$\beta$ -TCP	HAp	$\beta$ -TCP
0	0.9422 (3)	1.0431 (2)	0.6892 (2)	3.739 (2)	99.6 (5)	97.3 (5)
5	0.9423 (3)	1.0429 (3)	0.6892 (2)	3.740 (3)	99.5 (5)	96.2 (6)
30	0.9421 (3)	1.0428 (3)	0.6890 (2)	3.738 (2)	61.0 (5)	61.7 (5)
60	0.9420 (3)	1.0430 (4)	0.6889 (2)	3.741 (3)	49.3 (5)	53.3 (4)
240	0.9420 (3)	1.0431 (3)	0.6882 (2)	3.739 (2)	29.1 (5)	32.3 (5)
480	0.9435 (3)	1.0441 (5)	0.6884 (2)	3.738 (3)	26.6 (5)	29.6 (5)

PLLA have relatively small intensities and are not very notable in the diffractogram of the composite before the mechanical milling.

Concerning the part of the diffractograms characteristic for BCP, in addition to the widening of HAp diffraction lines issued by the decrease of the crystallites size during the mechanical treatment, no other significant changes were observed.

The size of crystallites and the cell parameters have been determined from the width of the diffraction line and Debye-Scherrer formula.

Table 1 shows calculated values of the cell parameters of the average particle of the ceramic component (HAp and  $\beta$ -TCP) in the BCP/PLLA composite before and after milling treatment. Calculated cell parameters are in accordance with literature values (JCPDS 9-432,  $a = b = 0.9418$  nm,  $c = 0.6884$  nm for HAp and JCPDS 09-169,  $a = b = 1.0429$  nm,  $c = 3.738$  nm for  $\beta$ -TCP).<sup>28,29</sup> From the displayed data (Table 1) it is concluded that no significant change of cell parameters values of the ceramic component in BCP/PLLA composite occurs during the mechanical treatment.

Table 1 also shows the effect of milling time on the size of crystallites of the ceramic component (HAp and  $\beta$ -TCP). These diagrams show the propensity of the size of crystallites to decrease with the prolonging of the mechanical treatment period. The sizes of crystallites decrease from 99.6 to 26.6 nm for HAp and from 97.3 to 29.6 nm for  $\beta$ -TCP.

### 3.2 Differential scanning calorimetry analysis (DSC)

Rearrangement and crystallization of PLLA on the HAp particle surfaces during composite preparation change the melting temperature of PLLA, its enthalpy and crystallinity.<sup>11</sup> The changes in these parameters were caused by rearrangement of the polymer chains near the filler and a change in the density of the packing of the polymer chains.<sup>9</sup>

DSC measurements (curves) of untreated and mechanically treated samples of BCP/PLLA composite are shown in Fig. 3. DSC curves give information about changes occurring in the PLLA phase of BCP/PLLA composite during milling. They show phase transitions characteristic of pure semi-crystalline PLLA: glass transitions (1), crystallization (2), and melting (3).

Each DSC curve exhibits a small exothermic peak of crystallization, followed by a single endothermic peak of melting, as is typical for PLLA.<sup>30</sup>

Apart from certain similarities, DSC curves shown in Fig. 3 have significantly different shapes, positions, and peak areas compared to the molten BCP/PLLA composite

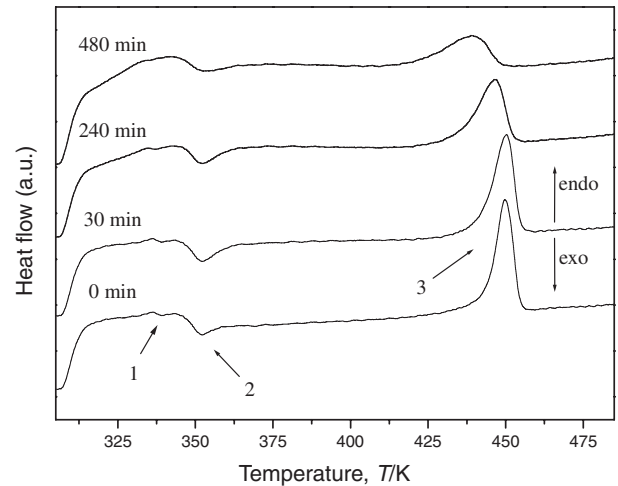


Fig. 3 Corresponding DSC curves of the mechanically treated BCP/PLLA samples according to the time of treatment.

Table 2 Thermal properties measured by DSC.

Milling time, <i>t</i> /min	$T_m$ /K	$\Delta H_m$ /Jg <sup>-1</sup>	$T_c$ /K	$\Delta H_c$ /Jg <sup>-1</sup>
0	449.8	54.9	352	14.8
30	450.3	54.5	352	14.5
240	446.4	47.2	352	11.5
480	438.8	33.7	352	10.9

biomaterial, which is the result of structural changes in the phase of PLLA caused by mechanical milling. The inorganic phase (BCP) is stable in the analyzed temperature range. Increased milling time causes a reduction of PLLA melting temperature ( $T_m$ ) in the composite (Fig. 3, Table 2).

Table 2 shows the changes of the thermal properties of PLLA in BCP/PLLA composite biomaterial measured by DSC as a function of the time of mechanical milling. By increasing the time of mechanical milling, the melting temperature and melting enthalpy of the polymer decrease. There was no variation in the crystallization temperature.

There are many relatively similar ways of calculating the crystallinity,  $\chi_c$ , of PLLA using DSC presented in existing literature.<sup>12,30-34</sup> In this study, crystallinity was calculated by

$$\chi_c(\%) = \frac{\Delta H_M - \Delta H_C}{\text{enthalpy}(100\% \text{cryst PLLA})} \cdot 100$$

where enthalpy of melting ( $\Delta H_M$ ) and the enthalpy of crystallization ( $\Delta H_C$ ) are proportional to the degree of

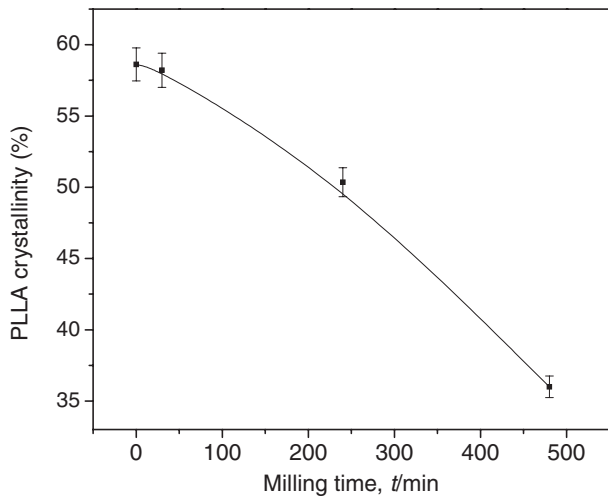


Fig. 4 Crystallinity of PLLA in BCP/PLLA composite depending on the milling time.

crystallinity.<sup>34)</sup> The theoretical value of the melting enthalpy for completely crystalline PLLA is 93.7 J/g.<sup>12,30-33)</sup> The enthalpy of crystallization is proportional to the quantity of the crystalline part in the sample. A decrease in ( $\Delta H_c$ ) corresponded to an increase in small and imperfect crys-

tals.<sup>35)</sup> The changes of the crystallinity of PLLA are shown in Fig. 4.

Figure 4 shows crystallinity decreases from 42.8 to 24.3%, calculated on polymer mass. Extending the milling time decreases the total crystalline phase, so that in the final result there is an increase in the amorphous phases. It can be concluded that by extending the mechanical milling processing some basic biological properties (for instance, time of the bioresorption) of the BCP/PLLA composite can be projected. The surrounding particles of the ceramic component (BCP) combined with the energy entered during mechanical treatment induces significant stress in the molecular chains of PLLA.

Due to mechanical factors and breaking of chains there was a decrease in PLLA molecular weight during mechanical processing.<sup>36)</sup> This reflects on the crystallinity degree and given composite melting temperature. The most significant effects caused by milling are the changes in properties of PLLA in the BCP/PLLA composite biomaterial. The obtained melting enthalpy and crystallinity degree are considerably lower than those of BCP/PLLA composite biomaterial before milling. A decrease in crystallinity of the PLLA phase surrounding BCP particles under high pressure was reported earlier by Shikinami.<sup>31)</sup> Lower crystallinity of PLLA in the BCP/PLLA composite

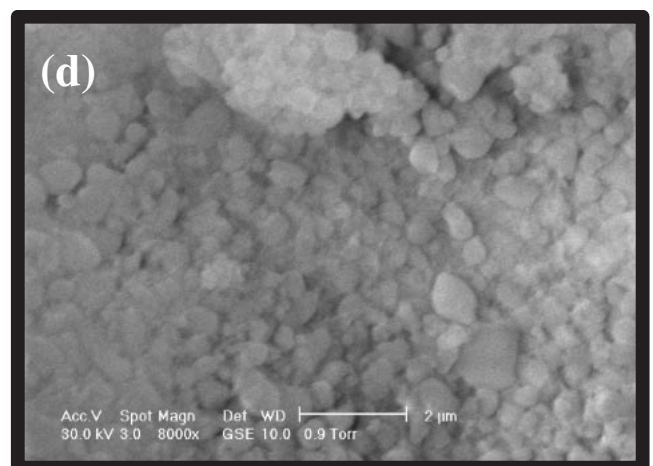
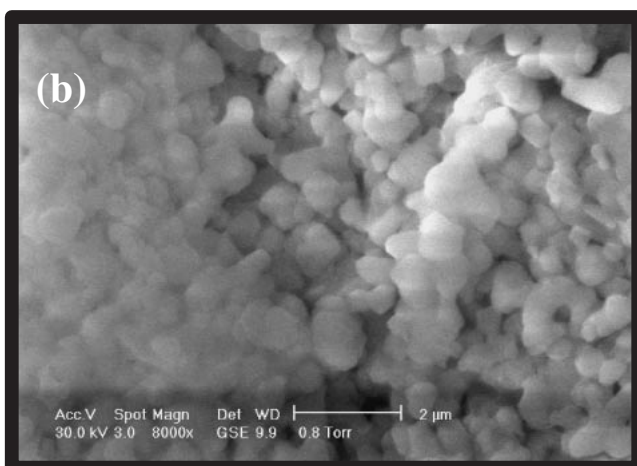
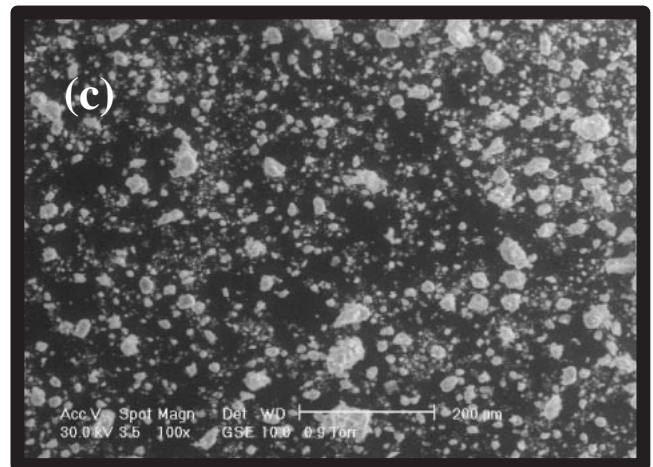
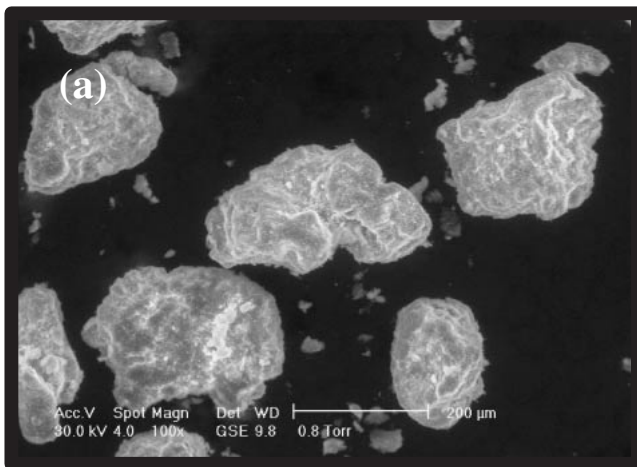


Fig. 5 ESEM showing BCP/PLLA composite: a), b) before the milling; c), d) after eight hours of milling.



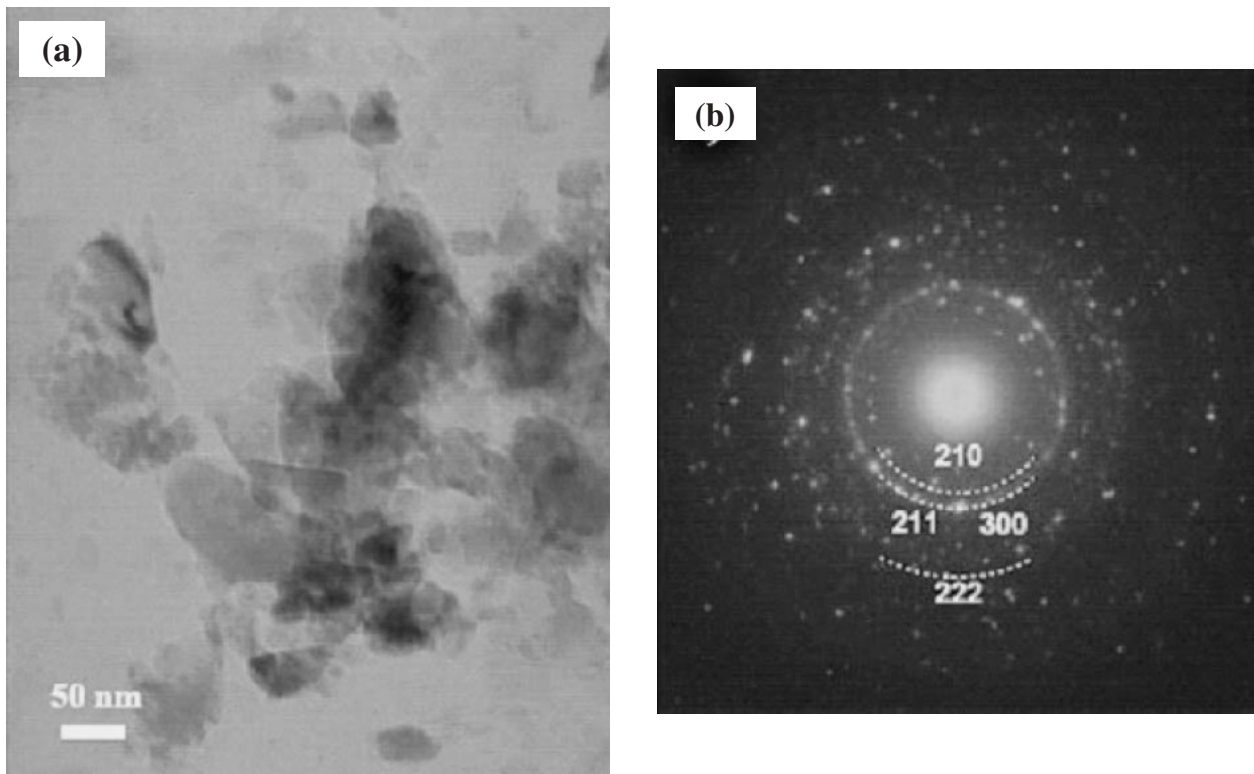


Fig. 6 TEM showing BCP/PLLA composite after eight hours of milling: a) fine particles of BCP, b) electron diffraction patterns of fine particles.

compared with pure PLLA and the formation of larger amorphous regions were found to occur due to separation and decrease in PLLA crystal regions caused by BCP particles under high pressure.

The application of this kind of material, with an increase of the amorphous phase in biological systems, would be noted by more intensive bioresorption in amorphous regions. Thus, the composite would show greater bioresorption.<sup>31)</sup>

### 3.3 Environmental scanning electronic microscopy (ESEM)

The surface microstructure of BCP/PLLA composite biomaterial before mechanical treatment is shown in Figs. 5(a) and 5(b). We can observe that crystallites of BCP (average size of around 70–95 nm) are connected with basic polymer matrix to form larger aggregates (average size of granules around 150–200  $\mu\text{m}$ ). Figures 5(c) and 5(d) show the surface microstructure of BCP/PLLA composite biomaterial after 8 h of mechanical milling. It is noticeable that average size of agglomerates of ceramic particles after milling is reduced to 5–20  $\mu\text{m}$ . The PLLA polymer matrix has not changed after the mechanical processing.

By comparing the ESEM images of the BCP/PLLA composite microstructure before and after 8 h of milling, it is concluded that during mechanical treatment, the composite becomes more homogeneous and ceramic particles are uniformly arranged in PLLA fine polymer matrix.

### 3.4 Transmission electron microscopy (TEM)

A high resolution image of BCP/PLLA particles after 8 h of mechanical treatment is shown in Fig. 6(a). Greater

amplification enables size evaluation of the individual particles. There are various particle sizes ranging from 30 to 50 nm. Results of crystallite size obtained by TEM are different from results obtained by XRD which is expected because of differences in these determination methods. Defining the grain size by XRD method is based on the number of approximations and it gives the mean value of the crystallites, while TEM method is based on the direct observance of the system and is closer to the real status. During TEM, the organic phase could not have been defined. This was probably due to the fact, that the high energy of the electron beam of the TEM (200 keV) causes the melting and decomposition of polylactide.<sup>11)</sup> Figure 6(b) also shows the electron diffraction patterns taken from the fine particles.

### 3.5 Infrared spectroscopy (IR)

IR spectroscopy was used to analyze any possible structural changes during mechanical milling. Figure 7 shows the comparative IR spectra of BCP/PLLA composite biomaterial before and after 8 h of mechanical treatment. The IR spectrum in Fig. 7(a) shows all characteristic bands for PLLA.<sup>37–41)</sup> The stretching mode of C=O group at 1755  $\text{cm}^{-1}$  is detected. The bending modes of CH<sub>3</sub> group at 1381 and 1451  $\text{cm}^{-1}$  and stretching modes of C-H group at 2994 and 2943  $\text{cm}^{-1}$  are also present. The IR spectrum in Fig. 7(b) shows all characteristic bands for HAp.<sup>37–41)</sup> The asymmetrical stretching ( $\nu_3$ ) modes at 1088 and 1048  $\text{cm}^{-1}$  and bending ( $\nu_4$ ) modes at 601 and 570  $\text{cm}^{-1}$  of the PO<sub>4</sub><sup>3-</sup> group were observed. The symmetrical stretching modes ( $\nu_1$  and  $\nu_2$ ) of PO<sub>4</sub><sup>3-</sup> group were also found at 957 and 473  $\text{cm}^{-1}$ . The liberation and stretching mode of the OH<sup>-</sup> was detected

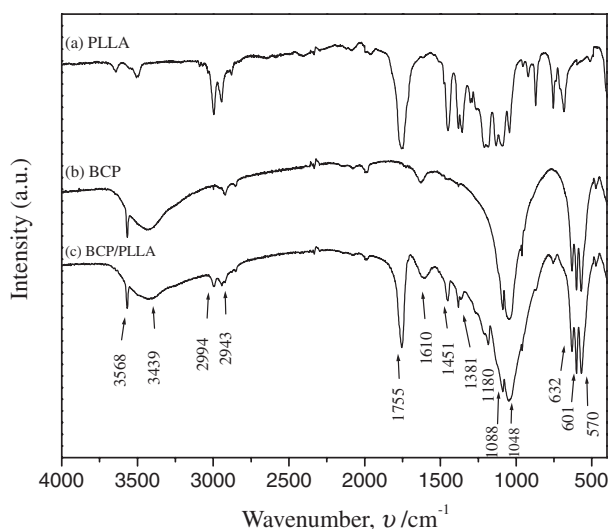


Fig. 7 Comparative IR spectrograms of a) PLLA; b) BCP and c) BCP/PLLA composite sample taken after 8 h of milling.

Table 3 Assignment of IR vibration bands of BCP/PLLA composite (\* $\nu$ -stretching vibrations, \* $\delta$ -bending vibrations).

Milling time (min)	BCP		PLLA	
	Vibration	Wavenumber (cm <sup>-1</sup> )	Vibration	Wavenumber (cm <sup>-1</sup> )
480	$\nu$ (PO <sub>4</sub> <sup>3-</sup> )	570		
	$\nu$ (PO <sub>4</sub> <sup>3-</sup> )	601	$\delta$ (C-H)	1381
	$\nu_L$ (OH)	632	$\delta$ (C-H)	1451
	$\nu$ (PO <sub>4</sub> <sup>3-</sup> )	1048	$\nu$ (C=O)	1755
	$\nu$ (PO <sub>4</sub> <sup>3-</sup> )	1088	$\nu$ (C-H)	2943
	$\nu$ (OH)	1610	$\nu$ (C-H)	2994
	$\nu$ (OH)	3568		

at 632 and 1610 cm<sup>-1</sup>, respectively. Absorption band at 3568 cm<sup>-1</sup> is also attributed to the OH<sup>-</sup> groups from HAp.

The spectrum of BCP/PLLA composite after 8 h of milling is given in Fig. 7c. All characteristic bands for PLLA and BCP are present (Table 3).

Table 3 shows the values of characteristic vibration bands of BCP/PLLA after 8 h of milling.

According to the IR spectra, after 8 h of milling, neither formation of new phases or disappearance of PLLA were recorded. In effect, no new absorption bands in the range of wave numbers from 400 to 4000 cm<sup>-1</sup> in the spectra of BCP/PLLA composite biomaterial after 8 h of milling, which confirms insignificant influence of milling on the appearance of degradation product of polymers (like oligomers or acetaldehyde).

#### 4. Conclusion

The analysis of mechanical processing of BCP/PLLA composite indicates the possibility to create specific properties in BCP/PLLA by applying mechanical treatment. The noticeable changes occur in the both constituent phases of BCP/PLLA composite during the mechanical treatment.

Based on X-ray analysis, increasing the time of mechanical

milling decreases the crystallite size of BCP. Milling time does not influence the values of cell parameters of HAp particles or  $\beta$ -TCP.

Analysis using DSC shows the changes of PLLA in composite caused by milling. An increased milling time causes a decrease in melting temperature and melting enthalpy of the polymer. There is also a decrease of PLLA crystallinity, which leads to a decrease in the total crystalline phase and an increase in the amorphous phases.

ESEM and TEM indicate that after 8 h of mechanical milling, the ceramic component of the composite becomes more homogeneous and particles are more uniformly arranged in the PLLA fine polymer matrix.

In the given time interval of mechanical treatment from 0 to 8 h, insignificant qualitative changes in the BCP and the PLLA phase were recorded by IR spectroscopy.

#### Acknowledgments

This work was supported by the Ministry of Science, Technology and Development of the Republic of Serbia, under Project No. 142006: Synthesis of functional materials with controlled structure on molecular and nano level. Authors are grateful to Dr Edin Suljovrujic and Prof Dr N. Cvjeticanin for their help in DSC and IR analysis.

#### REFERENCES

- 1) L. Hench: *J. Am. Ceram. Soc.* **81** (1998) 1705–1728.
- 2) N. Ignjatovic, S. Tomic, M. Dakic, M. Miljkovic, M. Plavšic and D. Uskokovic: *Biomaterials* **20** (1999) 809–816.
- 3) N. Ignjatovic, M. Plavšic, M. Miljkovic, Lj. Zivkovic and D. Uskokovic: *Journal of Microscopy* **196** (1999) 243–248.
- 4) S. N. Nazhat, M. Kellomaki, P. Tormala, K. E. Tanner and W. Bonfield: *J. Biomed. Mater. Res.* **58** (2001) 335–345.
- 5) N. Ignjatovic, K. Delijic, M. Vukcevic and D. Uskokovic: *Z. Metallkunde.* **92** (2001) 145–149.
- 6) S. Najman, Lj. Djordjevic, V. Savic, N. Ignjatovic and D. Uskokovic: *Bio-Medical Materials and Engineering* **14** (2004) 61–70.
- 7) N. Ignjatovic, M. Plavšic and D. Uskokovic: *Adv. Eng. Mater.* **2** (2000) 511–514.
- 8) Y. Shikinami, Y. Kotani, B. Cunningham, K. Abumi and K. Kaneda: *Adv. Funct. Mater.* **14** (2004) 1039–1046.
- 9) N. Bleach, S. Nazhat, K. Tanner, M. Kellomaki and P. Tormala: *Biomaterials* **23** (2002) 1579–1585.
- 10) R. Legeros, S. Lin, R. Rohanzadeh, D. Mijares and J. Legeros: *J. Mat. Sci.: Mater. M.* **14** (2003) 201–209.
- 11) N. Ignjatovic, E. Suljovrujic, J. Budimski, I. Krakovsky and D. Uskokovic: *J. Biomed. Mater. Res. Part B: Appl. Biomater.* **71B** (2004) 284–294.
- 12) A. Ignatius, S. Wolf, P. Augat and L. Claes: *J. Biomed. Mater. Res.* **57** (2001) 126–131.
- 13) C. Durucan and P. W. Brown: *J. Biomed. Mater. Res.* **51** (2000) 726–734.
- 14) N. Ignjatovic, K. Delijic, M. Vukcevic and D. Uskokovic: *Key Eng. Mater.* **192–195** (2001) 737–740.
- 15) Y. Shikinami and M. Okuno: *Biomaterials* **22** (2001) 3197–3211.
- 16) C. Verheyen, J. de Wijin, C. van Blitterswijk and K. de Groot: *J. Biomed. Mater. Res.* **26** (1992) 1277–1296.
- 17) E. Avvakumov, M. Senna and N. Kosova: *Soft Mechanochemical Synthesis*, (Kluwer Academic Publisher, 2001) pp. 20–85.
- 18) M. Meiti, T. Dellinger and P. Braun: *Adv. Funct. Mater.* **13** (2003) 795–799.
- 19) M. Trudeau, *Nanostructured Materials*, G. M. Chow and N. I. Noskova, (Eds., Kluwer Academic Publisher, 2002) pp. 10–62.
- 20) W. Suchanek, K. Byrappa, P. Shuk, R. Riman, V. Janas and K.

- TenHuisen: *J. Solid State Chemistry* **177** (2004) 793–799.
- 21) K. Yeong, J. Wang and S. Ng: *Biomaterials* **22** (2001) 2705–2712.
  - 22) I. Nikčević, V. Jokanović, M. Mitrić, Z. Nedić, D. Makovec and D. Uskoković: *J. Solid State Chemistry* **177** (2004) 2565–2574.
  - 23) S. Rhee: *Biomaterials* **23** (2002) 1147–1152.
  - 24) A. Yoshida, T. Miyazaki, E. Ishida and M. Ashizuka: *Mater. Trans.* **45** (2004) 994–998.
  - 25) R. Nemoto, S. Nakamura, T. Isobe and M. Senna: *Journal of Sol-Gel Science and Technology* **21** (2001) 7–12.
  - 26) L. Wang, E. Nemoto and M. Senna: *J. Mat. Sci.: Mater. M.* **15** (2004) 261–265.
  - 27) R. Rohanzadeh, M. Padrines, J. Bouler, D. Couchourel, Y. Fortun and G. Daculsi: *J. Biomed. Mater. Res.* **42** (1998) 530–539.
  - 28) JCPDS File No. 9-432, International Center for Diffraction Data.
  - 29) JCPDS file no. 09-169, International Center for Diffraction Data.
  - 30) J. Sarasua, R. Prudhomme, M. Wisniewski, A. Borghe and N. Spasky: *Macromolecules* **31** (1998) 3895–3905.
  - 31) Y. Shikinami and M. Okuno: *Biomaterials* **20** (1999) 859–877.
  - 32) H. Tsuju, T. Miyase, Y. Tezuka and S. Saha: *Biomacromolecules* **6** (2005) 244–254.
  - 33) L. Rodriguez-Lorenzo, A. Salinas, M. Vallet-Regi and J. San Roman: *J. Biomed. Mater. Res.* **30** (1996) 515–522.
  - 34) S. Sosnowski: *Polymer* **42** (2001) 637–643.
  - 35) M. Yasuniwa, S. Tsubakihara, Y. Sugimoto and C. Nakafuki: *Polym. Sci. Part B: Polym. Phys.* **42** (2004) 25–32.
  - 36) N. Ignjatović, E. Suljovrujić, Z. Stojanović and D. Uskoković: *Science of Sintering* **34** (2002) 79–93.
  - 37) S. Lazić, J. Katanic-Popović, S. Zec and N. Miljević: *Journal of Crystal Growth* **165** (1996) 124–128.
  - 38) N. Ignjatović, V. Savić, S. Najman, M. Plavsić and D. Uskoković: *Materials Science Forum* **352** (2000) 143–150.
  - 39) N. Ignjatović, V. Savić, S. Najman, M. Plavsić and D. Uskoković: *Biomaterials* **22** (2001) 571–575.
  - 40) R. A. Nyquist and R. O. Kagel: *Infrared Spectra of Inorganic Compounds*, (Academic Press, New York and London, 1971) pp. 12–42.
  - 41) K. Nakamoto: *Infrared and Raman Spectra of Inorganic and Coordination Compounds*, (John Wiley & Sons, New York, Chichester, Brisbane, Toronto, 1978) pp. 25–52.